J. Fluid Mech. (2014), *vol.* 740, *pp.* 5–16. © Cambridge University Press 2014
doi:10.1017/jfm.2013.626

Quantum vortex dynamics under the tangent representation of the local induction approximation

Robert A. Van Gorder†

Department of Mathematics, University of Central Florida, Orlando, FL 32816-1364, USA

(Received 14 August 2013; revised 2 November 2013; accepted 21 November 2013;
first published online 10 January 2014)

We derive the local induction approximation (LIA) for a quantum vortex filament in the arclength coordinate frame where the tangent vector is the unknown function. The equation for the tangent vector to the filament is then converted to a potential form, which ends up being a type of nonlinear Schrödinger equation that governs the tangential LIA model (T-LIA). Such a formulation was previously derived by Umeki for the standard fluid model (in the absence of superfluid friction terms). While it is challenging to generalize many of the exact solutions found for the standard LIA to the quantum LIA model, we demonstrate that the T-LIA model facilitates this generalization nicely. Indeed, under the T-LIA model, we are able to construct a variety of solutions. The Hasimoto solution related to elastica is one of the fundamental solutions present for the standard fluid model; however, using the T-LIA model, we are able to demonstrate the existence of such a solution, thereby extending the Hasimoto solution to the superfluid case. In the zero-temperature limit, purely self-similar solutions are shown to exist for the T-LIA model. As the superfluid warms (so that the influence of the normal flow is no longer negligible), the analogue to the self-similar solution is a new class of solutions, which depend on the similarity variable as well as a time-dependent additive scaling. In other words, the self-similar structures gradually deform as the magnitude of the normal-fluid velocity increases, which makes complete physical sense. When dealing with small deviations from the central axis of alignment, we can describe such solutions analytically. There exists a family of helical vortex filaments in the presence of a normal fluid impinging on the vortex, in complete agreement with the previously studied results for the LIA model. Finally, a number of soliton solutions are shown to exist in different regimes of the T-LIA model.

Key words: vortex dynamics, vortex flows, quantum fluids

1. Introduction

The self-induced velocity of a vortex in the reference frame moving with a superfluid under the local induction approximation (LIA) (Schwarz 1985) is given in non-dimensional form by

$$\boldsymbol{v} = \gamma\kappa\boldsymbol{t} \times \boldsymbol{n} + \alpha\boldsymbol{t} \times (\boldsymbol{U} - \gamma\kappa\boldsymbol{t} \times \boldsymbol{n}) - \alpha'\boldsymbol{t} \times (\boldsymbol{t} \times (\boldsymbol{U} - \gamma\kappa\boldsymbol{t} \times \boldsymbol{n})), \tag{1.1}$$

† Email address for correspondence: rav@knights.ucf.edu

https://doi.org/10.1017/jfm.2013.626 Published online by Cambridge University Press

where $\boldsymbol{U}$ is the dimensionless normal-fluid velocity, $\boldsymbol{t}$ and $\boldsymbol{n}$ are the unit tangent and unit normal vectors to the vortex filament, κ is the dimensionless average curvature, $\gamma = \Gamma \ln(c/\kappa a_0)$ is a dimensionless composite parameter (Γ is the dimensionless quantum of circulation, c is a scaling factor of order unity, $a_0 \approx 1.3 \times 10^{-8}$ cm is the effective core radius of the vortex), α and α' are dimensionless friction coefficients which are small (except near the λ-point; for reference, the λ-point is the temperature ($\approx$2.17 K, at atmospheric pressure) below which normal-fluid helium transitions to superfluid helium). This is the model of Schwarz, where the full Biot-Savart law has been replaced with the LIA, and hence is an approximation of the HVBK theory (Hall & Vinen 1956*a*,*b*; Bekarevich & Khalatnikov 1961) which disregards the mutual interaction of vortex filaments and vortex reconnections. See also the recent review of Nemirovskii (2013). Table 1 of Schwarz (1985) shows that at temperature $T = 1$ K we have $\alpha = 0.005$ and $\alpha' = 0.003$, while at temperature $T = 1.5$ K we have $\alpha = 0.073$ and $\alpha' = 0.018$. In the limit $(\alpha, \alpha') \to (0, 0)$, we recover the classical Da Rios equations for the motion of a vortex filament in a standard fluid (Da Rios 1906; Arms & Hama 1965; Ricca 1991). In keeping both parameters α and α' small yet non-zero, we ensure that the model accounts for superfluid friction. We shall refer to the model in the limit $\alpha, \alpha' \to 0$ as the standard fluid model, whereas we shall refer to the $\alpha > 0$, $\alpha' > 0$ case as the quantum LIA model. If we rescale time and the normal-fluid velocity, we may remove the factor of γ from (1.1). We shall do so in the subsequent derivations.

Perhaps the most standard form of the LIA and quantum LIA models is the curvature-torsion form, which is one type of intrinsic form. A natural extrinsic form could be the Cartesian form of these models (Boffetta *et al.* 2009; Van Gorder 2012*a*), which has the advantage of yielding vortex filament solutions which are easily viewed geometrically. A less studied form of the LIA was derived by Umeki (2010), who put the LIA into a form strictly involving the tangent vector to a filament. The resulting vector partial differential equation (PDE) admits a natural potential form, resulting in a new type of nonlinear Schrödinger equation (where the space variable is arclength). One very natural benefit of such an approach was that certain solutions become much easier to represent, with even closed-form solutions possible (Van Gorder 2012*b*; Umeki 2013).

Due to the fact that this formulation appears very natural for the LIA, it is reasonable to apply such a tangent-arclength formulation to the quantum LIA model, and this shall be our focus. We derive two explicit potential forms of this tangent-LIA (T-LIA) model. In § 2, we consider the low-temperature limit when the influence of $\boldsymbol{U}$ is negligible, and demonstrate the existence and properties of two very fundamental solutions: planar filaments (along the lines of the Hasimoto solution related to elastica) and self-similar structures. In § 3, we include the effects of the normal-fluid velocity $\boldsymbol{U}$, and demonstrate the existence of helical and soliton solutions, which are driven by the normal-fluid velocity. In addition, we determine the manner in which self-similar structures are disrupted under the inclusion of the normal-fluid impinging on the quantum vortex. So, the T-LIA model is shown to be useful for understanding the qualitative structure of a variety of quantum LIA solutions.

2. Formulation including normal and binormal friction

In the low-temperature limit, the influence of the normal fluid impinging on the filament is often neglected, so we set $U \to 0$, where U is the magnitude of the normal-fluid velocity $\boldsymbol{U}$. This condition is vacuously satisfied when $\alpha, \alpha' \to 0$, and this

https://doi.org/10.1017/jfm.2013.626 Published online by Cambridge University Press

limit corresponds to the zero-temperature limit. Svistunov (1995) explored this case, and Boffetta *et al.* (2009) proposed a model in Cartesian coordinates. Many studies on specific structures in the quantum LIA model have taken the normal-fluid velocity to zero, as it permits one to study such structures without the influence of drift or other distorting effects on the filaments (Vinen 2001; Araki, Tsubota & Nemirovskii 2002; Alamri, Youd & Barenghi 2008). The physical applicability of such a scenario is limited to the very low-temperature regime, in superfluid helium 4, and many more papers consider the $U \neq 0$ case: see Baggaley, Laurie & Barenghi (2012). However, in the case of superfluid helium 3, the normal-fluid velocity U is zero (because helium 3 is very viscous, unlike helium 4, so it is always at rest or in solid-body rotation, but α and α' are not zero). Relevant experiments have been done in Lancaster and Helsinki by Fisher and co-workers and Eltsov and co-workers respectively (see Eltsov *et al.* 2008; Fisher & Pickett 2009).

Setting $U = 0$, differentiating with respect to the arclength variable s, and performing several vector manipulations, the quantum LIA model (1.1) becomes

$$\dot{\boldsymbol{t}} = \frac{\partial}{\partial s}\left\{(1-\alpha'|\boldsymbol{t}|^2)\boldsymbol{t}\times\boldsymbol{t}_s - \alpha[(\boldsymbol{t}\cdot\boldsymbol{t}_s)\boldsymbol{t} - |\boldsymbol{t}|^2\boldsymbol{t}_s]\right\}. \tag{2.1}$$

We have also rescaled relevant quantities to remove the γ factor. Forcing $\boldsymbol{t}$ to be a unit tangent vector, the equation simplifies slightly to

$$\dot{\boldsymbol{t}} = \frac{\partial}{\partial s}\left\{(1-\alpha')\boldsymbol{t}\times\boldsymbol{t}_s - \alpha[(\boldsymbol{t}\cdot\boldsymbol{t}_s)\boldsymbol{t} - \boldsymbol{t}_s]\right\}. \tag{2.2}$$

This gives us a representation of the quantum LIA dynamics strictly in terms of the tangent vector to the filament, $\boldsymbol{t}$. Next, we introduce the potential function $v \in \mathbb{C}$, where for $\boldsymbol{t}(t, x) = (t_1(x, t), t_2(x, t), t_3(x, t))$ we set

$$t_1 + \mathrm{i}t_2 = \frac{2v}{1+|v|^2}, \quad t_3 = \frac{1-|v|^2}{1+|v|^2}. \tag{2.3}$$

This v is the same potential function as used by Umeki in the standard fluid ($\alpha = \alpha' = 0$) case. We obtain (scaling $t \mapsto (1-\alpha')t$)

$$\mathrm{i}v_t + v_{ss} - \frac{2v_s^2 v^*}{1+|v|^2} - \hat{\alpha}\mathrm{i}\left[v_{ss} - \frac{2v_s^2 v^*}{1+|v|^2} - \frac{4vv_sv_s^*}{1-|v|^4}\right] = 0, \tag{2.4}$$

where $\hat{\alpha} = \alpha/(1-\alpha')$. This formulation is a clear generalization of the Umeki formulation of the standard LIA (Umeki 2010). Indeed, taking $\alpha, \alpha' \to 0$, we recover that model. It was shown that the Umeki formulation admits several exact solutions (Umeki 2013).

We should note that while a plane wave of the form $v(s, t) = A\mathrm{e}^{\mathrm{i}(ks-\omega t)}$ exists for the standard LIA (even in the arclength form; see Umeki 2013), such a simple solution cannot exist for the model (2.4). The reason for this discrepancy is that such a helical solution's development is fundamentally associated with the normal-fluid velocity (Van Gorder 2013*a*). In § 3, we shall show that including a non-zero magnitude for the normal-fluid velocity allows us the existence of a family of helical filaments.

2.1. *Perturbation of the planar filament due to superfluid friction terms*

A planar vortex filament is one of the important general forms of a vortex filament which can be given analytically (Kida 1981), and was first done so by Hasimoto (1971). This solution can even be scaled, so as to obtain more interesting

https://doi.org/10.1017/jfm.2013.626 Published online by Cambridge University Press

planar filaments depending on functional arguments (Van Gorder 2013*b*). Even then, extending such a filament to the quantum LIA model is complicated analytically in the curvature-torsion and Cartesian frameworks. However, as demonstrated in Van Gorder (2012*b*), in the arclength frame, such a solution can be given in a rather elegant form in the case of a standard fluid. Therefore, it makes sense to use the arclength formulation of the Hall–Vinen model in order to determine if such an extension of this planar filament can exist.

A planar filament in the Umeki formulation takes the form of a stationary state $v(s,t) = \mathrm{e}^{-\mathrm{i}\omega t} q(s)$. In Van Gorder (2012*b*), it was shown that an exact solution exists for the $\hat{\alpha} = 0$ case and takes the form

$$v(s,t) = \mathrm{e}^{-\mathrm{i}\omega t} q_\omega(s) = A\mathrm{e}^{-\mathrm{i}\omega t}\ \mathrm{sn}\left(\sqrt{\frac{\omega}{1+A^2}}(s-s_0), A\mathrm{i}\right). \tag{2.5}$$

If we assume a first-order perturbation solution, we find that the order-one correction is purely complex, that is $v(s,t) = \mathrm{e}^{-\mathrm{i}\omega t}[q_\omega(s) + \mathrm{i}\hat{\alpha} Q(s)]$, where $Q(s)$ satisfies

$$\omega Q + Q'' + \frac{2{q'_\omega}^2 Q - 4q'_\omega q_\omega Q'}{1+q_\omega^2} = q''_\omega + \frac{2{q'_\omega}^2 q_\omega}{1-q_\omega^2}. \tag{2.6}$$

The first-order correction due to $\hat{\alpha}$ then takes the form

$$Q(s) = -q_\omega(s)\int_0^s \frac{\left(1+q_\omega(\zeta)^2\right)^2}{q_\omega(\zeta)^2}\int_0^\zeta \frac{4q_\omega(\xi)^2 q'_\omega(\xi)^2 + \omega q_\omega(\xi)(1-q_\omega(\xi)^4)}{\left(1+q_\omega(\xi)^2\right)^3\left(1-q_\omega(\xi)^2\right)}\,\mathrm{d}\xi\,\mathrm{d}\zeta. \tag{2.7}$$

The modified form of the planar vortex filament due to the superfluid friction parameters is then

$$\begin{aligned} v(s,t) = \mathrm{e}^{-\mathrm{i}\omega t} q_\omega(s)\Bigg[1 - \mathrm{i}\hat{\alpha}\int_0^s \frac{\left(1+q_\omega(\zeta)^2\right)^2}{q_\omega(\zeta)^2} \\ \times \int_0^\zeta \frac{4q_\omega(\xi)^2 q'_\omega(\xi)^2 + \omega q_\omega(\xi)(1-q_\omega(\xi)^4)}{\left(1+q_\omega(\xi)^2\right)^3\left(1-q_\omega(\xi)^2\right)}\,\mathrm{d}\xi\,\mathrm{d}\zeta\Bigg], \end{aligned} \tag{2.8}$$

where $q_\omega(s)$ is the Jacobi sn function defined in (2.5).

Some notes are in order. The qualitative change in the planar filament is primarily due to α and not α', and α' is often neglected and set to zero in the literature. We see from the planar vortex filament that the first-order correction due to α is rather drastic, highlighting the complications in extending the LIA to the superfluid case.

As A goes to zero, note that the first-order correction (2.7) does not diverge. The inner integral scales as A, the outer integral gives a contribution of at worst order A^{-2}, so performing both integrations we have a term of order at worst A^{-1}. The factor $q_\omega(s)$ outside of the integral gives another multiplicative factor of A, and thus the first-order correction (2.7) is (at worst) of order $O(1)$ as A tends toward zero. Actually performing the integrations for the appropriately defined $q_\omega(s)$, we find that the correction should go as order A. This makes sense, as the correction should tend toward zero as the unperturbed parent term goes to zero. Another way to more easily see this is to consider (2.6) directly when A is small. This gives $\omega Q + Q'' = Aq''_\omega(s) + O(A^2)$. The correction can be shown to then take the form

$$Q(s) = \frac{A}{\sqrt{\omega}}\int_0^s \sin\left(\sqrt{\omega}[s-\xi]\right) q''_\omega(\xi)\,\mathrm{d}\xi. \tag{2.9}$$

https://doi.org/10.1017/jfm.2013.626 Published online by Cambridge University Press

Physically, the inclusion of superfluid friction parameters disrupts the planar filament in such a way that the resulting filament curves or bends so that it no longer lies on a plane. Indeed, while the unperturbed filament lies along a plane described by $(\cos(t), \sin(t))$ for any t (the plane itself rotates), the stationary part of the perturbed solution is complex (with non-trivial real and imaginary parts) which means that the solution no longer lies on a plane.

It is natural to wonder if such filaments are spectrally stable. The planar filament in the standard fluid LIA is orbitally stable (as was shown numerically (Kida 1982) and analytically (Van Gorder 2013*c*)); however this deformation of the planar filament is not simply a perturbed solution to the same nonlinear Schrödinger equation. Rather, the entire governing equation is changed (for $\alpha > 0$), so we are dealing with a structural perturbation of the problem as well. Hence, the question of stability is not as simple as treating the solution (2.5) as a perturbation of (2.8). Rather, such a stability analysis should be performed on general perturbations of solutions to (2.4) directly.

2.2. *Purely self-similar filament structures*

Similarity solutions (solutions which maintain their form independent of scale) have been considered for the curvature-torsion and Cartesian reference frames in the absence of a normal fluid impinging on the filament. Lipniacki (2003*a*,*b*) demonstrated self-similarity for a version of the local induction equation where the dependent quantities were curvature and torsion (this is the classical intrinsic coordinate frame). Similar results were obtained in the Cartesian frame of reference quite recently (Van Gorder 2013*d*). For a mathematical treatment of similarity solutions in the curvature-torsion reference frame, see Gutiérrez, Rivas & Vega (2003). The case studied therein was for the standard fluid model, corresponding to the $\alpha, \alpha' \to 0$ limit (i.e. the zero-temperature limit). In all of these studies, $U = 0$ was taken, which is consistent with the low-temperature regime (Vinen 2001; Araki *et al.* 2002; Lipniacki 2003*a*,*b*; Alamri *et al.* 2008).

Let us take the similarity variable $\eta = s/\sqrt{t}$ and the similarity solution $v(s, t) = g(\eta)$. The potential equation (2.4) reduces to

$$-\frac{\mathrm{i}}{2}\eta g' + g'' - \frac{2g'^2 g^*}{1+|g|^2} - \hat{\alpha}\mathrm{i}\left[g'' - \frac{2g'^2 g^*}{1+|g|^2} - \frac{4g|g'|^2}{1-|g|^4}\right] = 0, \tag{2.10}$$

where a prime denotes differentiation with respect to the similarity variable. From here one can separate real and imaginary parts of g and solve numerically. In order to determine the qualitative properties of the solution dependence on $\hat{\alpha}$, we shall consider a small-amplitude solution (corresponding to a vortex filament with small deviation in s and t). Doing so, we neglect terms of order two or higher, obtaining the linearized expression

$$-\frac{\mathrm{i}}{2}\eta g' + (1 - \hat{\alpha}\mathrm{i})g'' = 0. \tag{2.11}$$

We find that

$$g'(\eta) = \epsilon \exp\left(-\frac{\hat{\alpha}}{1+\hat{\alpha}^2}\eta^2\right)\left\{\cos\left(\frac{\eta^2}{1+\hat{\alpha}^2}\right) + \mathrm{i}\sin\left(\frac{\eta^2}{1+\hat{\alpha}^2}\right)\right\}, \tag{2.12}$$

https://doi.org/10.1017/jfm.2013.626 Published online by Cambridge University Press

where ϵ is a small parameter of the order of magnitude of the small-amplitude solution. From here, we recover the approximation to the small-amplitude solution,

$$g(\eta) = \delta_1 + \epsilon \int_0^\eta \cos\left(\frac{\nu^2}{1+\hat{\alpha}^2}\right) \exp\left(-\frac{\hat{\alpha}\nu^2}{1+\hat{\alpha}^2}\right) \mathrm{d}\nu + \mathrm{i}\left[\delta_2 + \epsilon \int_0^\eta \sin\left(\frac{\nu^2}{1+\hat{\alpha}^2}\right) \exp\left(-\frac{\hat{\alpha}\nu^2}{1+\hat{\alpha}^2}\right) \mathrm{d}\nu\right], \tag{2.13}$$

where δ_1, δ_2 are sufficiently small parameters. So, in the absence of the normal fluid, purely self-similar filament structures can exist.

What we have therefore shown is that, in the absence of a normal fluid impinging on the vortex, there exist filament structures which are completely self-similar in nature. These self-similar structures are completely determined by (2.10). In the situation where deviations of the filament from a reference axis are small, the self-similar filaments can be approximated according to formula (2.13).

In terms of the physics of the problem, the existence of such solutions implies that, in the low-temperature limit where $U \to 0$, well-organized structures are possible. The natural scaling for the similarity goes as $x \sim \sqrt{t}$. At large length and time scales, the solutions mirror their behaviour at small time scales. For small deviations from a central axis, the behaviours are manifested as solutions which oscillate about this central axis, at all scales. This self-similarity is rather idealized. In the following section, we shall see what is preserved of the self-similarity when a non-zero normal-fluid velocity is introduced. Fonda *et al.* (2012) demonstrate the agreement of the self-similar solutions obtained under LIA with experiments on Kelvin waves (at a temperature of 1.98 K).

3. Formulation including normal-fluid flow

For larger temperatures, the normal fluid impinging on the vortex matters qualitatively, and should be included. On the other hand, the friction parameter α' does not influence the behaviour of the solutions strongly (much less so than α), and shall be neglected in this section. One may write $\boldsymbol{U} = U\boldsymbol{t} + U_a\boldsymbol{n} + U_b\boldsymbol{b}$ where $\boldsymbol{b}$ is the binormal vector. As discussed in Shivamoggi (2013), the transverse velocity components U_a and U_b often result in an algebraic rescaling of the Kelvin waves along the filament, while U (the velocity component along the filament) influences the filament in a qualitative manner. Therefore, we consider consider $U \neq 0$ and $U_a = U_b = 0$ to determine the qualitative features of the filament solutions to the quantum LIA model. Umeki (2013) developed a transformation between the Cartesian LIA and the arclength LIA variables. Making use of this transformation, we can derive the arclength form of the quantum LIA model including the normal fluid, through the Cartesian form of the quantum LIA model. We find that, upon setting $\alpha' = 0$ and differentiating (1.1) with respect to s, the quantum LIA model becomes (making use of the same potential function v as defined in (2.3))

$$\mathrm{i}v_t + v_{ss} - \frac{2v_s^2 v^*}{1+|v|^2} - \alpha\mathrm{i}\left[v_{ss} - \frac{2v_s^2 v^*}{1+|v|^2} - \frac{4vv_s v_s^*}{1-|v|^4}\right] - \alpha U\left(\frac{1+|v|^2}{1-|v|^2}\right)^2 v_s = 0, \tag{3.1}$$

where the final term is the influence due to the normal fluid impinging on the vortex. If the magnitude of the normal-fluid velocity is small, it is sufficient to consider the results of the previous section. On the other hand, if the magnitude of U is large, the final term is more dominant than the term involving only α. The model is most useful

https://doi.org/10.1017/jfm.2013.626 Published online by Cambridge University Press

when perturbations along the vortex filament are small. When they are large, one may wish to use the full form of the quantum LIA given in (1.1).

3.1. *Helical filaments*

Unlike in the zero-normal-flow case, when $U \neq 0$ there exists an exact planar wave solution to (3.1). Such a solution is manifested as a helical structure when plotted in the coordinate frame (t_1, t_2). Assuming $v(s, t) = A \exp(\mathrm{i}[kx - \omega t])$, we have

$$\omega - k^2 + \frac{2A^2k^2}{1+A^2} - \alpha \mathrm{i}\left[\left(\frac{1+A^2}{1-A^2}\right)k^2 - U\left(\frac{1+A^2}{1-A^2}\right)^2 k\right] = 0. \tag{3.2}$$

Separating real and imaginary parts, $\omega = ((1-A^2)/(1+A^2))k^2$, $A = \sqrt{(k-U)/(k+U)}$, so $\omega = kU$. The solution is then

$$v(s, t) = \sqrt{\frac{k-U}{k+U}}\mathrm{e}^{\mathrm{i}k(x-Ut)}. \tag{3.3}$$

Note that while this solution does not explicitly depend on the superfluid friction parameter, α, it does require that $\alpha > 0$, which yields a unique value of the amplitude A. This solution also requires $k > U$. On the other hand, if $\alpha = 0$, the amplitude would not be specified, so there would exist an infinite family of solutions, one for each value of $A \in (0, 1)$. In that case, the solution does not involve U.

The existence of such a helical structure is to be expected. Such solutions naturally exist in the Cartesian frame of reference. In the zero-temperature limit of the Cartesian frame, helical filaments were studied by Sonin (2012). More recently, helical filament solutions for the positive temperature case (which includes $\alpha > 0$ and $\alpha' > 0$) have also been studied (Van Gorder 2013*a*). Like in the Cartesian frame (Van Gorder 2013*a*), there exists a relation between the permitted region for the wavenumber and the magnitude of the normal-fluid velocity. In particular, if the magnitude of the normal-fluid velocity is high, the vortex filament exists only if the wavenumber is sufficiently large. In other words, there can be no slowly rotating helical vortices in the presence of strong normal-fluid flow.

The exact solution (3.3) also demonstrates that this rotating helix cannot exist for $U = 0$. Indeed, in the absence of a normal-fluid contribution, we would be left with a helix $v(s, t) = \mathrm{e}^{\mathrm{i}ks}$. However, such a helix is time-independent (so there can be no rotation). Such a standing solution would be highly unlikely for the physical problem. Hence, the rotation helical solution is actually driven by the normal-fluid flow. There is no explicit dependence on α, in complete agreement with the Cartesian formulation (Van Gorder 2013*a*). However, the existence of this solution does depend on $\alpha > 0$; from (3.2), if $\alpha > 0$, then we may determine the exact form of the amplitude in terms of k and U. Without such a specification, the amplitude of the helix is undetermined.

3.2. *A soliton in the small-amplitude regime when the normal-fluid flow dominates*

One of the more famous solutions for the standard fluid LIA is the Hasimito 1-soliton (Hasimoto 1972). However, finding such a general soliton in the quantum LIA model in either the curvature-torsion or Cartesian frames has not been done, due to the added complication of the highly nonlinear terms associated with superfluid friction. If one is willing to linearize such equations, it is possible to obtain locally stationary structures which behave as solitary waves (Shivamoggi 2011, 2013).

https://doi.org/10.1017/jfm.2013.626 Published online by Cambridge University Press

Let us now consider a soliton in the small-α, large-U limit where (3.1) reduces to

$$\mathrm{i}v_t + v_{ss} - \frac{2v_s^2 v^*}{1+|v|^2} - \alpha U\left(\frac{1+|v|^2}{1-|v|^2}\right)^2 v_s = 0. \tag{3.4}$$

In particular, consider $v(s,t) = \exp(-\mathrm{i}\omega\alpha^2U^2t)p(S)$, where $S = \alpha Us$. The resulting equation is rather complicated to solve, even numerically. Under the assumption of a small-amplitude solution, with $\epsilon \ll 1$ the maximal deviation of the filament from the reference axis, we find (neglecting terms of nonlinearity order greater than three) that

$$\omega p + \frac{\mathrm{d}^2p}{\mathrm{d}S^2} - 2p\left(\frac{\mathrm{d}p}{\mathrm{d}S}\right)^2 - (1+4p^2)\frac{\mathrm{d}p}{\mathrm{d}S} = 0. \tag{3.5}$$

The choice of ω is ours, since we use it as a scaling parameter. In the case of $\omega = -6$, we have $p(S) = \epsilon \mathrm{e}^{-2S}$ as an exact solution. So, when deviations from the reference axis are small, we have soliton solutions which scale like $v(s,t) = \epsilon\exp(6\mathrm{i}\alpha^2U^2t)\exp(-2S) = \epsilon\exp(6\mathrm{i}\alpha^2U^2t)\exp(-2\alpha Us)$ for $s \geqslant 0$. Such solutions have maximal amplitude at zero arclength and gradually decay as the arclength becomes large. Therefore, the time evolution of a small soliton-type perturbation localized at $s = 0$ can be determined in the case where U dominates α, that is, for the case of strong normal-fluid flow. Note that, in the Cartesian geometry, one can view $s = 0$ as occurring at a wall. As s increases and one moves away from the wall, the filament gradually decays to a straight line filament.

3.3. *A soliton in the intermediate regime*

For the intermediate regime, where neither small α nor large U dominate, it is still possible to seek a soliton solution. Assume $v(s,t) = \exp[-(\omega_1 + \mathrm{i}\omega_2)\alpha^2U^2t]p(S)$, where $S = \alpha Us$. Note that the time dependence is no longer only a phase contribution. For solutions to remain bounded in time, it is necessary that $\omega_1 > 0$. We again assume small deviations from the reference axis, of magnitude $\epsilon \ll 1$. The equation governing p then becomes

$$\begin{aligned}(\omega_2 - \mathrm{i}\omega_1)p + (1-\alpha\mathrm{i})\frac{\mathrm{d}^2p}{\mathrm{d}S^2} - 2(1-\alpha\mathrm{i})p^*\left(\frac{\mathrm{d}p}{\mathrm{d}S}\right)^2 \\ + 4\alpha\mathrm{i}p\frac{\mathrm{d}p}{\mathrm{d}S}\left(\frac{\mathrm{d}p}{\mathrm{d}S}\right)^* - (1+4|p|^2)\frac{\mathrm{d}p}{\mathrm{d}S} = 0.\end{aligned} \tag{3.6}$$

It makes sense to seek a solution $p(S) = \epsilon\exp[(r_1 + \mathrm{i}r_2)S]$. We obtain an algebraic system of four equations for the four unknowns ω_1, ω_2, r_1 and r_2, resulting in the solution

$$\begin{aligned}v(s,t) = \epsilon\exp\left(\frac{6\mathrm{i}\alpha U}{1+9\alpha^2}\left[s + \alpha U\frac{1+\alpha^2}{1+9\alpha^2}t\right]\right) \\ \times \exp\left(-\frac{2\alpha U}{1+9\alpha^2}\left[s + \alpha^2U\frac{13+45\alpha^2}{1+9\alpha^2}t\right]\right).\end{aligned} \tag{3.7}$$

What we see is that, in the intermediate regime (where neither α nor U dominates), the soliton solution decays both as arclength and time increase. This is in contrast to the soliton in the large-U regime, where there is only decay for large s and persistence of a non-zero perturbation for all time. Hence, in this intermediate case, the filament asymptotically decays so that is has no deviation from the reference axis, as $t \to \infty$.

https://doi.org/10.1017/jfm.2013.626 Published online by Cambridge University Press

Furthermore, due to the damping term involving α, as α increases in value the soliton decays more rapidly.

3.4. *Quasi-similarity solution with temporal drift*

For non-zero U, there is not a pure similarity solution. The breakdown of self-similarity in the $U \neq 0$ case was previously highlighted in Van Gorder (2013*d*). However, there does exist a transformation which maps a pseudo-similarity solution into the similarity solution obtained for the $U = 0$ case. Let us consider a solution of the form $v(s,t) = h(\zeta)$, where $\zeta = \eta + \chi(t)$ and $\eta = s/\sqrt{t}$ is the similarity variable introduced before. Neglecting terms of order two or higher (valid for small deviations from the centralized axis),

$$-\frac{\mathrm{i}}{2}\zeta h' + (1-\alpha\mathrm{i})h'' + \left(\frac{\mathrm{i}}{2}\chi'(t) + \mathrm{i}\chi(t) - \alpha U\sqrt{t}\right)h' = 0. \tag{3.8}$$

When the rightmost term is zero, this equation reduces to an equation of the form (2.11). This, in turn, means that the function χ must satisfy the first-order ordinary differential equation $(\mathrm{i}/2)\chi'(t) + \mathrm{i}\chi(t) - \alpha U\sqrt{t} = 0$, the solution of which reads

$$\chi(t) = -2\mathrm{i}\alpha U\left\{\sqrt{t} - \sqrt{2}F\left(\sqrt{\frac{t}{2}}\right)\right\}, \quad \text{where } F(\sigma) = \mathrm{e}^{-\sigma^2}\int_0^\sigma \mathrm{e}^{\xi^2}\,\mathrm{d}\xi \tag{3.9}$$

is Dawson's integral. Therefore, for filaments with small deviation from the centralized axis, we have that $h(\zeta) = g(\zeta)$, g is the function given in (2.12) (which will need to have real and imaginary parts regrouped) and

$$\zeta = \eta - 2\mathrm{i}\alpha U\left\{\sqrt{t} - \sqrt{2}F\left(\sqrt{\frac{t}{2}}\right)\right\} = \frac{s}{\sqrt{t}} - 2\mathrm{i}\alpha U\left\{\sqrt{t} - \sqrt{2}F\left(\sqrt{\frac{t}{2}}\right)\right\}. \tag{3.10}$$

Thus, we have obtained a variation of the pure similarity solution given in the previous section, which includes the influence of the non-zero normal-fluid velocity. The influence of the normal-fluid velocity is to induce a sort of drift term, which adds a temporal correction to the similarity variable.

Since $\alpha \ll 1$, and the correction to η is of the order $\sqrt{t}$, the similarity solutions are disrupted only for large time scales. For the small time scales (when the solution is like that of the purely self-similar case), the filaments remain bounded for all t and all s. However, for large time scales, the similarity solutions give way to solutions involving the composite variable ζ. If s is particularly large, the influence of the correction is small. However, for time scales much larger than the arclength scale, the correction dominates. The growth of this correction is like $O(t^{1/2})$, while the decay of the similarity part of ζ goes like $O(t^{-1/2})$.

4. Conclusions

We obtain the quantum LIA model in terms of the tangent vector to the vortex filament. Under an appropriate transformation, this vector PDE is put into potential form, resulting in a type of nonlinear Schrödinger equation (NLS). This is in analogy with the result of Umeki (2010) for the LIA. We demonstrate that this formulation is actually rather useful, as it permits us to construct a number of solutions analytically. Many of these solutions (the planar, helical, and self-similar filaments) were known for the standard LIA, yet had not been analytically extended to the quantum LIA model in the presence of superfluid friction or a normal fluid impinging on the filament.

https://doi.org/10.1017/jfm.2013.626 Published online by Cambridge University Press

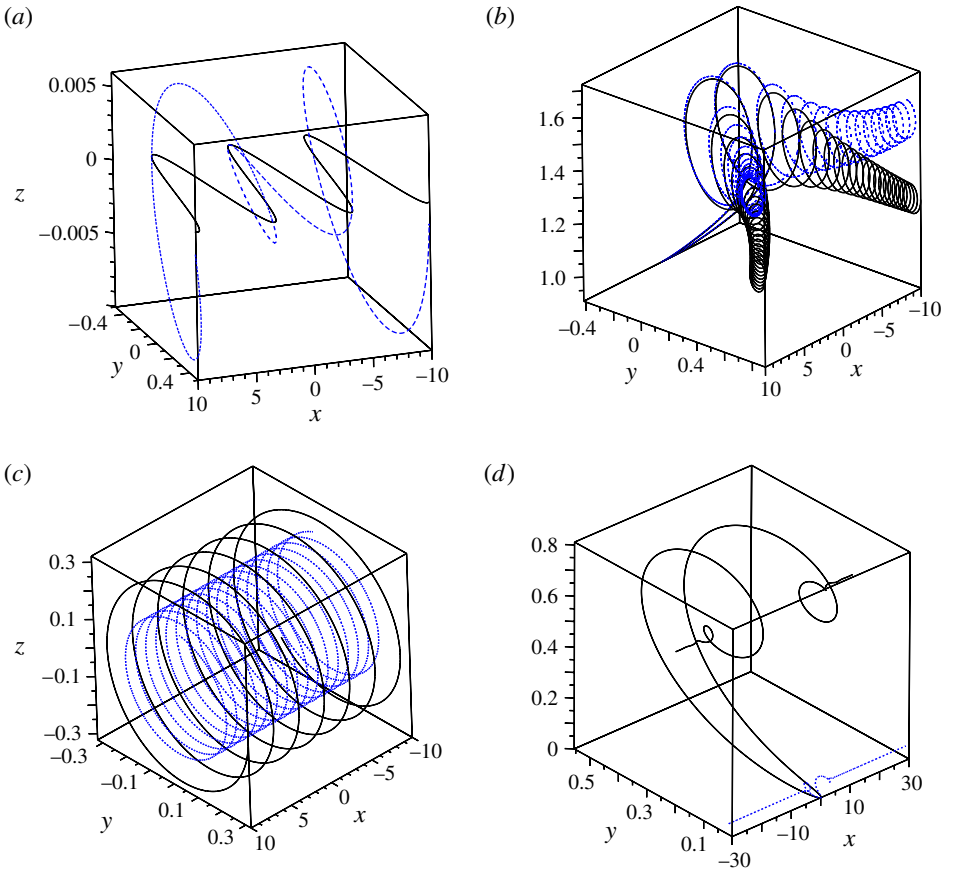


FIGURE 1. (Colour online) Plots of solutions obtained over Cartesian space at fixed time. In (*a*) we demonstrate the deformation of planar filaments due to superfluid friction as given analytically by (2.8). The solid line represents $\alpha = \alpha' = 0$, while the dashed line represents $\alpha = 0.005$, $\alpha' = 0.003$. In (*b*) we plot (numerically) the self-similar solutions for $\alpha = \alpha' = 0$ (solid line), $\alpha = 0.005$, $\alpha' = 0.003$ (dashed line) corresponding to the fully nonlinear equation (2.10). In (*c*) we plot helical solutions for $U = 1$, $k = 2$ (solid line) and $U = 1$, $k = 5$ (dashed line). As the wavenumber k increases, the period increases while the amplitude in (Cartesian coordinates) decreases. Soliton solutions (3.7) are given in (*d*), for $\alpha = 0.005$ (solid black line) and $\alpha = 0.073$ (dashed line) in the presence of a normal fluid ($U = 1$). The perturbation size of these soliton excitations of the tangent filament is $\epsilon = 0.01$ (though the corresponding value of the perturbation is much larger in the Cartesian frame).

Additionally, some solitary wave perturbations were constructed, which model soliton Kelvin waves along the filament. Note that we considered two reductions of the quantum LIA equation (1.1), namely (2.4) and (3.1), each of which models a qualitatively distinct situation.

The primary utility in using the tangent form of the quantum LIA model developed here lies in the fact that it permits one to construct solutions, either analytically or numerically, with relative ease, since the quantum LIA model is put into a potential equation which is a kind of NLS. The influence of both superfluid friction and the normal fluid are taken into account through such a model. The main drawback to this formulation is that the solutions are given for the tangent vector to the filament, as

https://doi.org/10.1017/jfm.2013.626 Published online by Cambridge University Press

opposed to a more obviously useful quantity. However, using the transformation of Umeki (2013), it is possible to map every solution obtained here into a solution in the Cartesian reference frame. It is noteworthy that this procedure is apparently simpler than attempting to obtain the solutions directly in the Cartesian frame, as the potential equation obtained there (Van Gorder 2012*a*) is not so simple to solve in the case of some of the filaments obtained here (for instance, the deformations of the planar filaments). In figure 1, we provide some of the solutions obtained here, after they have been mapped back to the Cartesian frame of reference. We demonstrate the effect of the superfluid friction parameters on the planar filament, the self-similar filament, the helical filament, and one of the soliton filaments.

One qualitative feature we notice is that solutions can essentially be separated into two groups: those which exist in the low-temperature limit ($U = 0$), and those which require $U > 0$. The former include the self-similar vortex filament; when $U \neq 0$, these filaments are strongly perturbed by the oncoming flow, resulting in a loss of pure self-similarity. On the other hand, the helical and soliton solutions of § 3 are driven by this flow. This becomes very clear when one considers the tangent form of the quantum LIA model.

Acknowledgements

The author was supported in part by NSF grant number no. 1144246. The author wishes to thank the anonymous referees, whose comments have led to definite improvement in the presentation of the results.

REFERENCES

ALAMRI, S. Z., YOUD, A. J. & BARENGHI, C. F. 2008 Reconnection of superfluid vortex bundles. *Phys. Rev. Lett.* **101**, 215302.

ARAKI, T., TSUBOTA, M. & NEMIROVSKII, S. K. 2002 Energy spectrum of superfluid turbulence with no normal-fluid component. *Phys. Rev. Lett.* **89**, 145301.

ARMS, R. J. & HAMA, F. R. 1965 Localized-induction concept on a curved vortex and motion of an elliptic vortex ring. *Phys. Fluids* **8**, 553.

BAGGALEY, A. W., LAURIE, J. & BARENGHI, C. F. 2012 Vortex-density fluctuations, energy spectra, and vortical regions in superfluid turbulence. *Phys. Rev. Lett.* **109**, 205304.

BEKAREVICH, I. L. & KHALATNIKOV, I. M. 1961 Phenomenological derivation of the equations of vortex motion in He II. *Sov. Phys. JETP* **13**, 643.

BOFFETTA, G., CELANI, A., DEZZANI, D., LAURIE, J. & NAZARENKO, S. 2009 Modelling Kelvin wave cascades in superfluid Helium. *J. Low Temp. Phys.* **156**, 193.

DA RIOS, L. S. 1906 Sul moto d'un liquido indefinite con un filetto vorticoso di forma qualunque. *Rend. Circ. Mat. Palermo* **22**, 117.

ELTSOV, V. B., DE GRAAF, R., HÄNNINEN, R., KRUSIUS, M. & SOLNTSEV, R. E. 2008 Experiments on the twisted vortex state in superfluid ^{3}He-B. *J. Low Temp. Phys.* **150**, 373.

FISHER, S. N. & PICKETT, G. R. 2009 Quantum turbulence in superfluid ^{3}He at very low temperatures. *Prog. Low Temp. Phys.* **16**, 147–194.

FONDA, E., MEICHLE, D. P., OUELLETTE, N. T., HORMOZ, S., SREENIVASAN, K. R. & LATHROP, D. P. 2012 Visualization of Kelvin waves on quantum vortices, arXiv:1210.5194.

GUTIÉRREZ, S., RIVAS, J. & VEGA, L. 2003 Formation of singularities and self-similar vortex motion under the localized induction approximation. *Commun. Pure Diff. Equ.* **28**, 927.

HALL, H. E. & VINEN, W. F. 1956*a* The rotation of liquid helium II. I. Experiments on the propagation of second sound in uniformly rotating helium II. *Proc. R. Soc. Lond.* A **238**, 204.

HALL, H. E. & VINEN, W. F. 1956*b* The rotation of liquid helium II. II. The theory of mutual friction in uniformly rotating helium II. *Proc. R. Soc. Lond.* A **238**, 215.

https://doi.org/10.1017/jfm.2013.626 Published online by Cambridge University Press

HASIMOTO, H. 1971 Motion of a vortex filament and its relation to elastica. *J. Phys. Soc. Japan* **31**, 293.

HASIMOTO, H. 1972 A soliton on a vortex filament. *J. Fluid Mech.* **51**, 477.

KIDA, S. 1981 A vortex filament moving without change of form. *J. Fluid Mech.* **112**, 397.

KIDA, S. 1982 Stability of a steady vortex filament. *J. Phys. Soc. Japan* **51**, 1655.

LANDAU, L. D. & LIFSHITZ, E. M. 1959 *Fluid Mechanics*. Addison and Wesley.

LIPNIACKI, T. 2003*a* Shape-preserving solutions for quantum vortex motion under localized induction approximation. *Phys. Fluids* **15**, 1381.

LIPNIACKI, T. 2003*b* Quasi-static solutions for quantum vortex motion under the localized induction approximation. *J. Fluid Mech.* **477**, 321.

NEMIROVSKII, S. K. 2013 Quantum turbulence: theoretical and numerical problems. *Phys. Rep.* **524**, 85 2.5.1.

RICCA, R. L. 1991 Rediscovery of Da Rios equations. *Nature* **352**, 561.

SCHWARZ, K. W. 1985 Three-dimensional vortex dynamics in superfluid ^{4}He: line–line and line–boundary interactions. *Phys. Rev.* B **31**, 5782.

SHIVAMOGGI, B. K. 2011 Vortex motion in superfluid ^{4}He: reformulation in the extrinsic vortex-filament coordinate space. *Phys. Rev.* B **84**, 012506.

SHIVAMOGGI, B. K. 2013 Vortex motion in superfluid ^{4}He: effects of normal fluid flow. *Eur. Phys. J.* B **86**, 275.

SONIN, E. B. 2012 Dynamics of helical vortices and helical-vortex rings. *Eur. Phys. Lett.* **97**, 46002.

SVISTUNOV, B. 1995 Superfluid turbulence in the low-temperature limit. *Phys. Rev.* B **52**, 3647.

UMEKI, M. 2010 A locally induced homoclinic motion of a vortex filament. *Theor. Comput. Fluid Dyn.* **24**, 383.

UMEKI, M. 2013 A real-space representation of a locally induced vortex filament. *Theor. Appl. Mech. Japan* **61**, 195.

VAN GORDER, R. A. 2012*a* Fully nonlinear local induction equation describing the motion of a vortex filament in superfluid ^{4}He. *J. Fluid Mech.* **707**, 585.

VAN GORDER, R. A. 2012*b* Exact solution for the self-induced motion of a vortex filament in the arclength representation of the local induction approximation. *Phys. Rev.* E **86**, 057301.

VAN GORDER, R. A. 2013*a* Motion of a helical vortex filament in superfluid ^{4}He under the extrinsic form of the local induction approximation. *Phys. Fluids* **25**, 085101.

VAN GORDER, R. A. 2013*b* Scaling laws and accurate small-amplitude stationary solution for the motion of a planar vortex filament in the Cartesian form of the local induction approximation. *Phys. Rev.* E **87**, 043203.

VAN GORDER, R. A. 2013*c* Orbital stability for rotating planar vortex filaments in the Cartesian and arclength forms of the local induction approximation. *J. Phys. Soc. Japan* **82**, 094005.

VAN GORDER, R. A. 2013*d* Self-similar vortex dynamics in superfluid ^{4}He under the Cartesian representation of the Hall–Vinen model including superfluid friction. *Phys. Fluids* **25**, 095105.

VINEN, W. F. 2001 Decay of superfluid turbulence at a very low temperature: the radiation of sound from a Kelvin wave on a quantized vortex. *Phys. Rev.* B **64**, 134520.

https://doi.org/10.1017/jfm.2013.626 Published online by Cambridge University Press